Electronic Supplementary Material (ESI) for Journal of Materials Chemistry

Supporting Information

One-dimensional Metal-Organic Framework Photonic Crystals Used as Platforms for Vapor Sorption

Florian M. Hinterholzinger,[a‡] Annekathrin Ranft,[b‡] Johann M. Feckl,[a] Bastian Rühle,[a] Thomas Bein[a] and Bettina V. Lotsch*[b]*

[a] *Department of Chemistry and Center for NanoScience (CeNS), University of Munich (LMU), Butenandtstrasse 11 (E), 81377 München (Germany), Phone: (+49)89218077621, Fax: (+49) 89-2180-77622, E-mail: bein@lmu.de, Homepage: http://www.cup.uni-muenchen.de/pc/bein*

[b] *Max Planck Institute for Solid State Research, Heisenbergstraße 1, 70569 Stuttgart (Germany) and Department of Chemistry and Center for NanoScience (CeNS), University of Munich (LMU), Butenandtstrasse 5-13 (D), 81377 München (Germany), Phone: : (+49)7116891611, Fax: (+49)7116891612 E-mail: b.lotsch@mpg.fkf.de, Homepage: http://www.cup.uni-muenchen.de/ac/lotsch/*

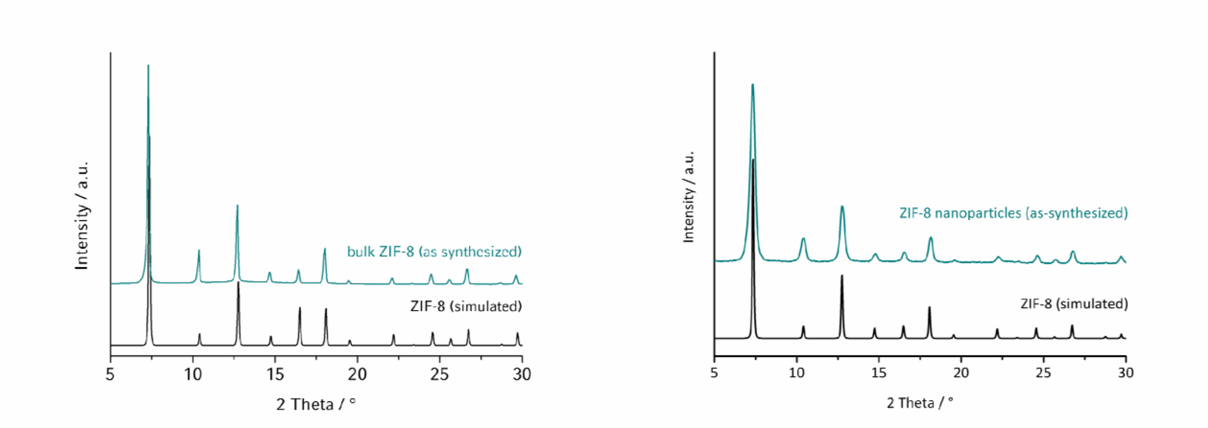

Figure S1: X-ray diffraction patterns (background corrected) of as-synthesized bulk ZIF-8 material (left) as well as of ZIF-8 nanoparticles (right) compared to simulated data.

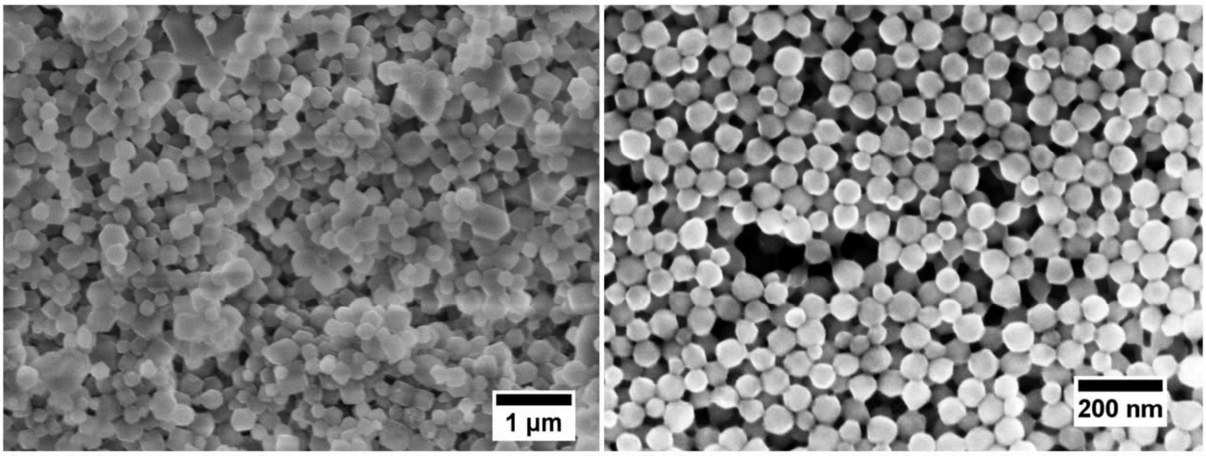

Figure S2: Scanning electron microscopy (SEM) images showing a bulk ZIF-8 powder sample obtained from the mixture solution used for the fabrication of **BS-1** (left) as well as ZIF-8 nanoparticles used for the preparation of **BS-2** (right).

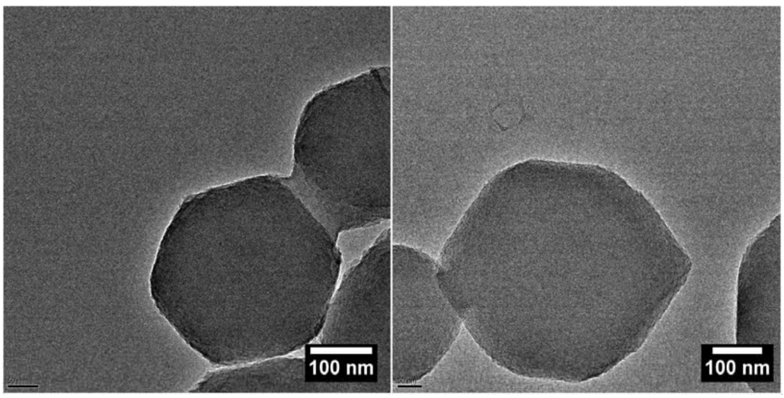

Figure S3: Transmission electron microscopy (TEM) micrographs showing as-synthesized ZIF-8 nanocrystals isolated from a powder sample obtained from the reaction solution used for dense ZIF-8 film growth.

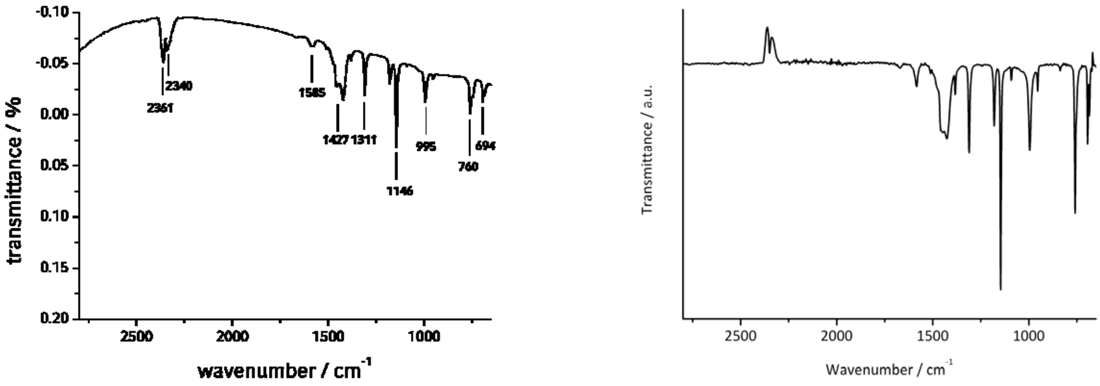

Figure S4: IR spectra of bulk ZIF-8 (left) as well as of ZIF-8 nanoparticles (right).

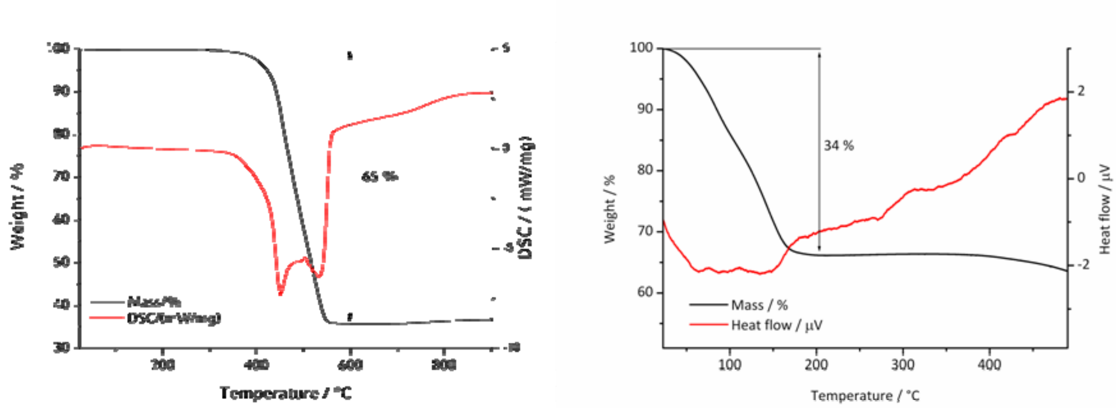

Figure S5: Thermogravimetric analysis (TGA), differential scanning calorimetry (DSC) and differential thermal analysis (DTA) of bulk ZIF-8 (left) and ZIF-8 nanoparticles (right), respectively, illustrating a one-step weight loss as well as the decomposition of bulk ZIF-8.

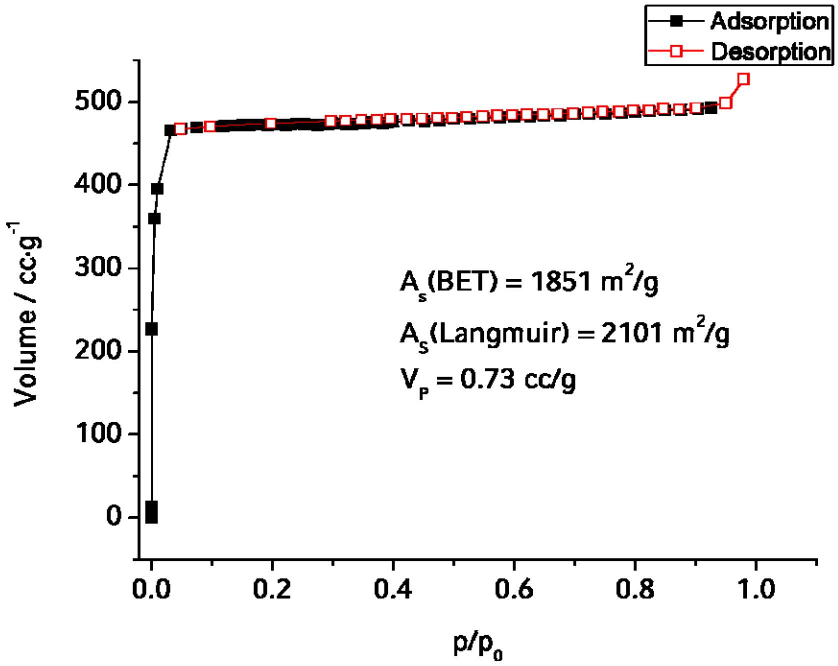

Figure S6: Physisorption measurement performed with nitrogen at 77 K for bulk ZIF-8 showing a type I isotherm, the specific surface area (BET/Langmuir) and the pore volume.

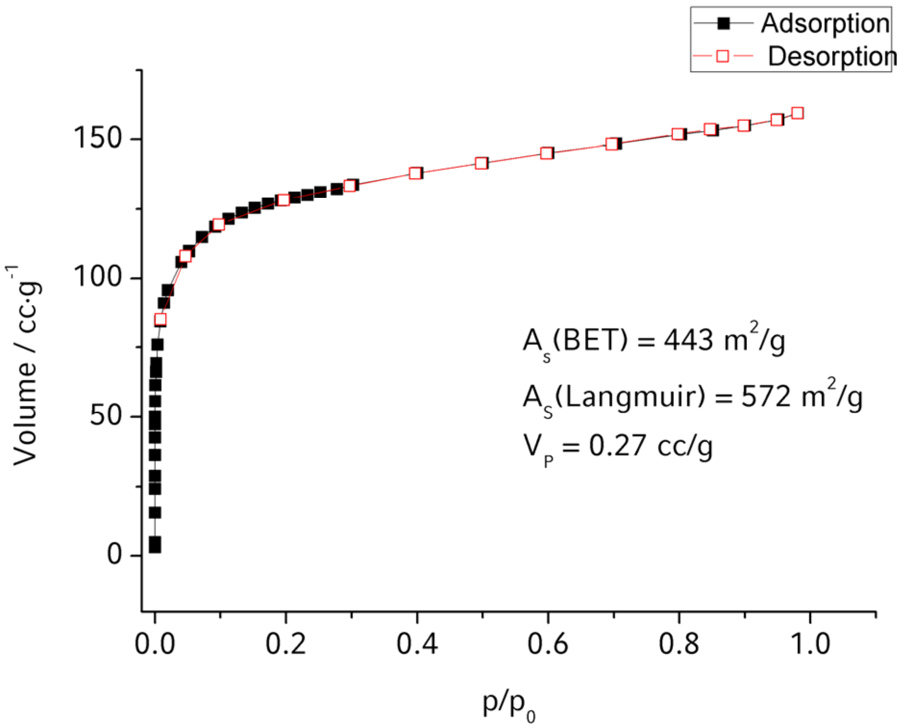

Figure S7: Physisorption measurement at 77 K performed on a titania nanoparticle sample synthesized without structure-directing agent (F127) showing a type I isotherm, the specific surface area (BET/Langmuir) and the pore volume.

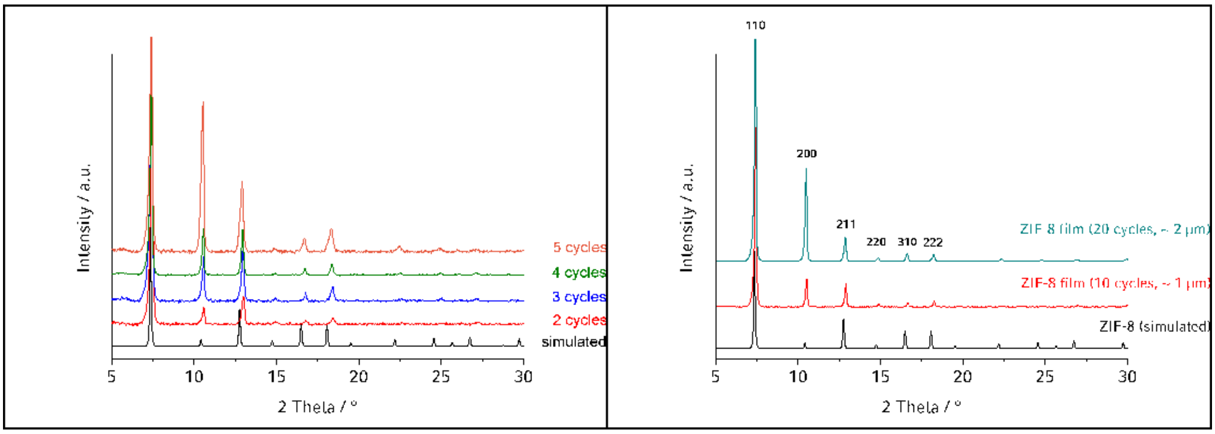

Figure S8: X-ray diffraction patterns (background corrected) of ZIF-8 thin films after different growing cycles compared to simulated data.

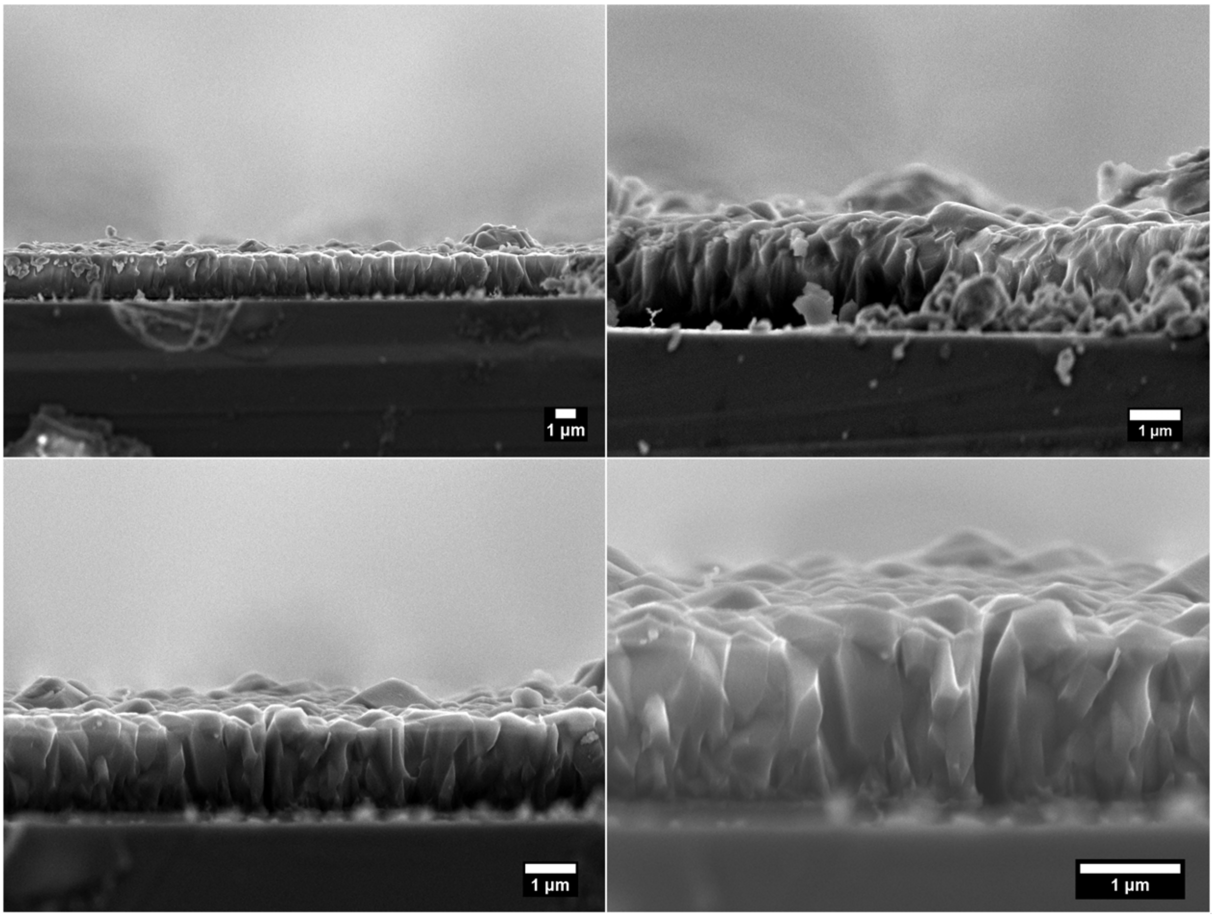

Figure S9: SEM micrographs showing a 10-cycled ZIF-8 thin film (magnification: x4.000 (top, left); x10.000 (top, right); x10.000 (bottom, left); x20.000 (bottom, right)).

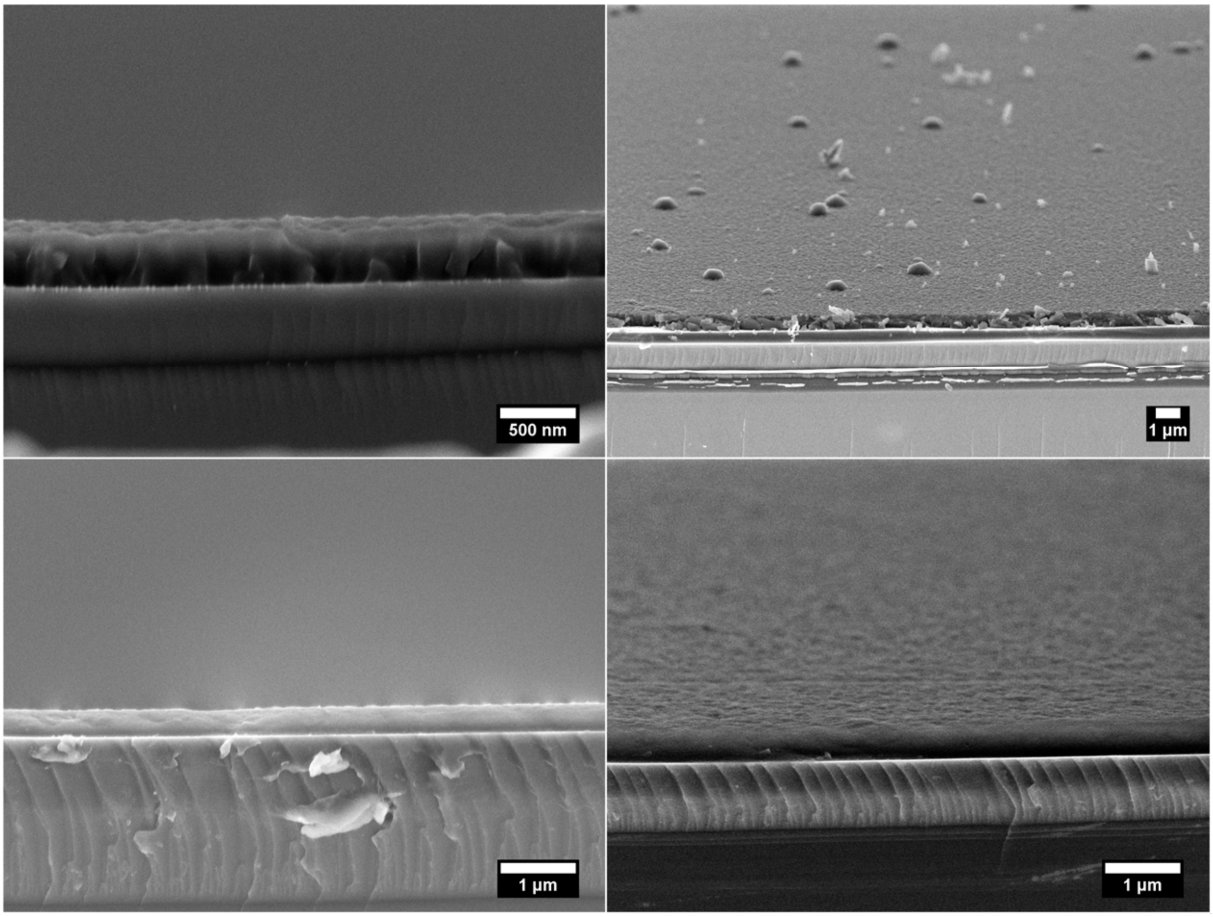

Figure S10: SEM micrographs showing ZIF-8 thin films grown in a crystallization solution while shaking (top) as well as under ultrasonic irradiation (bottom) (magnification: x5.000 (top, left); x30.000 (top, right); x15.000 (bottom, left); x15.000 (bottom, right)).

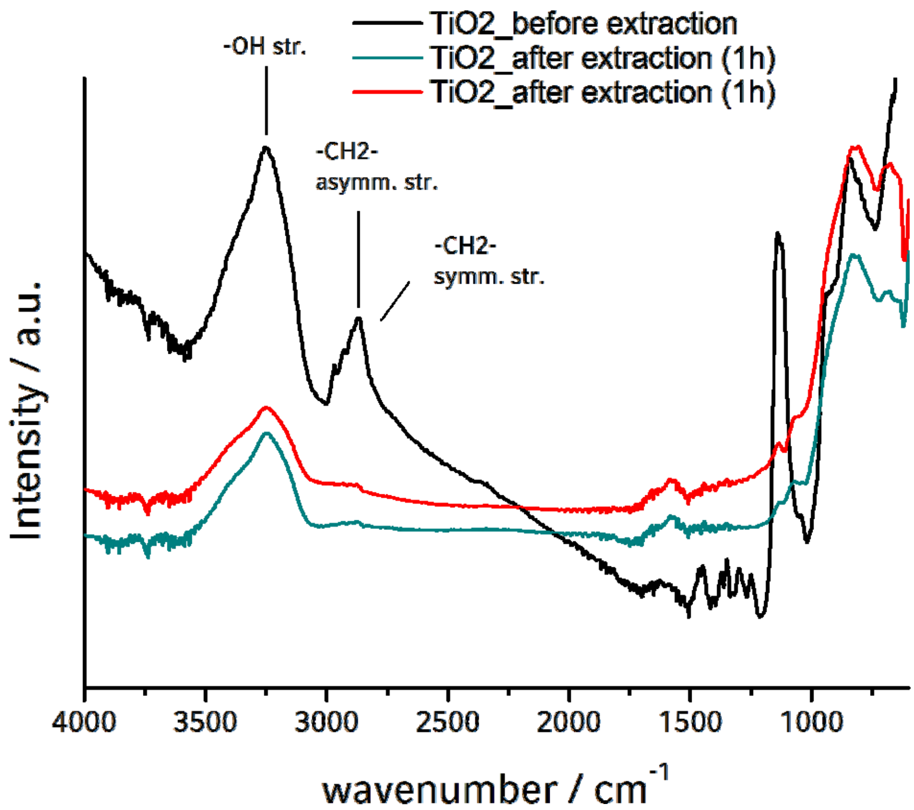

Figure S11: RAIR spectra of a TiO2 thin film before and after the ethanol extraction procedure.

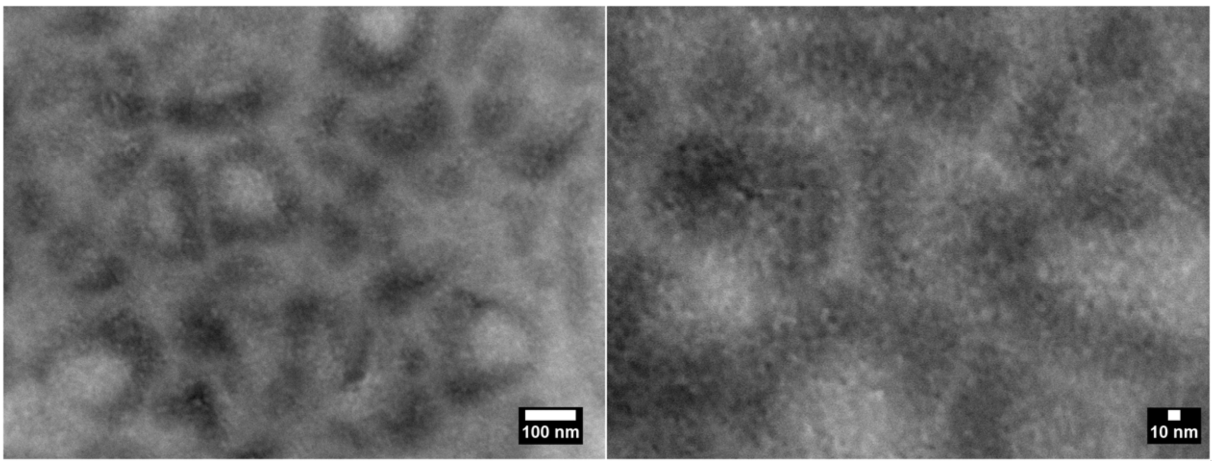

Figure S12: SEM micrographs demonstrating the mesoporous structure of a thin TiO_2 film after ethanol extraction (magnification: x100.000 (left); x250.000 (right)).

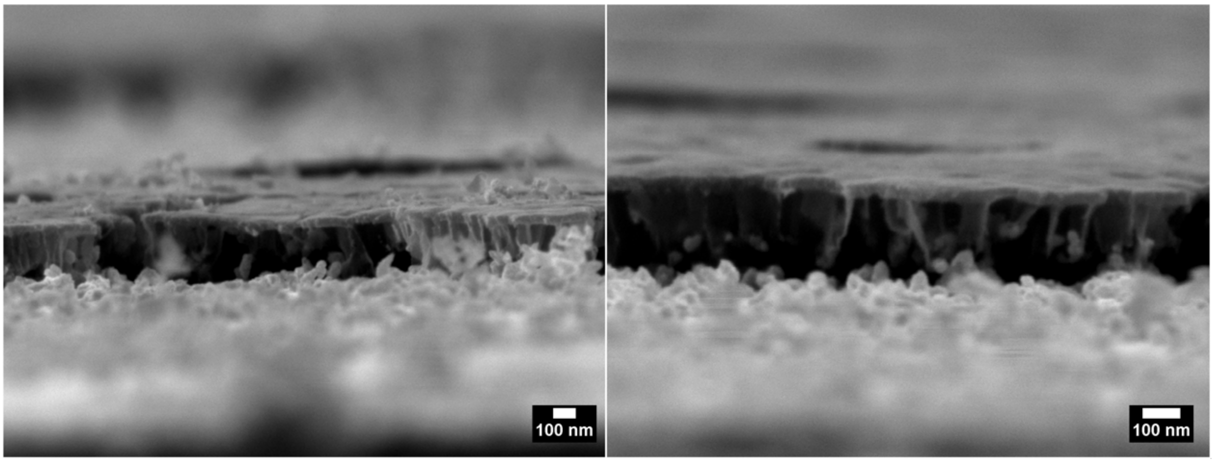

Figure S13: SEM micrographs showing bilayered Bragg stack-1 with an average film thickness of ~ 50 nm for each titania layer and ~ 200 nm for each ZIF-8 layer, respectively. The ZIF-8/mp-TiO2 Bragg stack is depicted for different magnifications (x45.000 (left); x75.000 (right)).

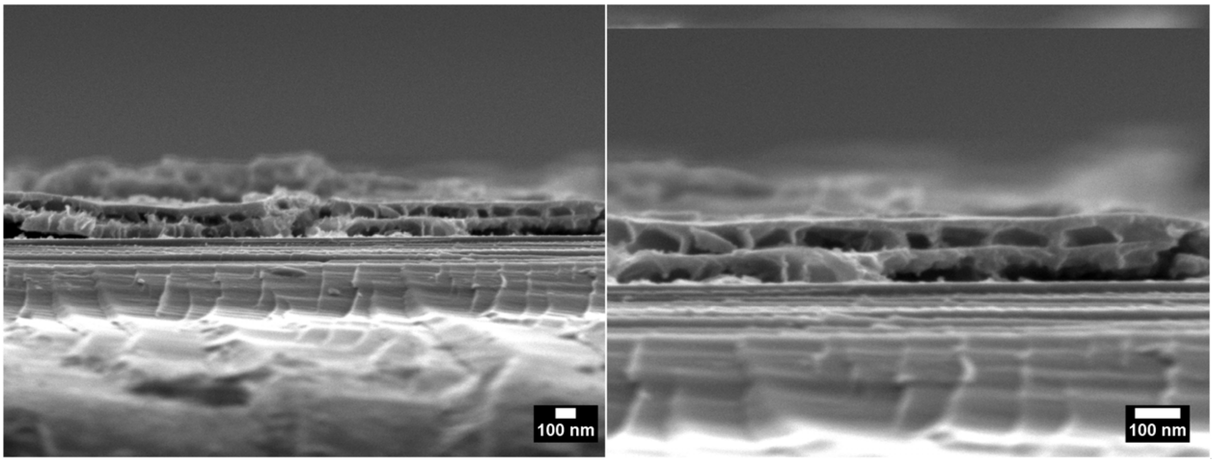

Figure S14: SEM micrographs showing the two bilayered Bragg stack-1 with an average film thickness of ~ 50 nm for each titania layer and ~ 70 nm for each ZIF-8 layer, respectively. The ZIF-8/mp-TiO2 Bragg stack is depicted for different magnifications (x40.000 (left); x90.000 (right)).

Electronic Supplementary Material (ESI) for Journal of Materials Chemistry

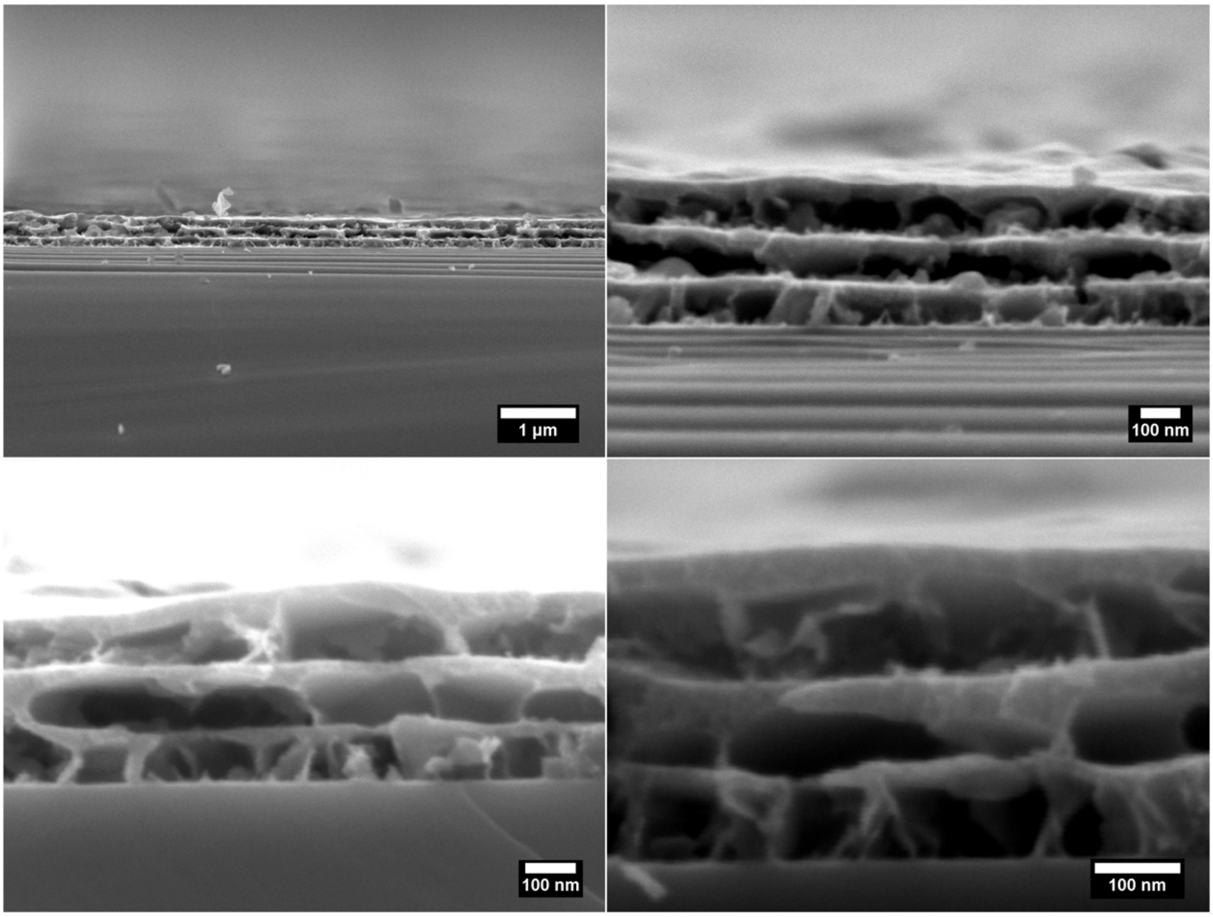

Figure S15: Scanning electron micrographs showing the 3 bilayered Bragg stack-1 with an average film thickness of ~ 50 nm for each titania layer and ~ 70 nm for each ZIF-8 layer, respectively. ZIF-8/mp-TiO_2 Bragg stack is depicted for different magnifications (x15.000 (top, left); x80.000 (top, right); x100.000 (bottom, left); x170.000 (bottom, right)).

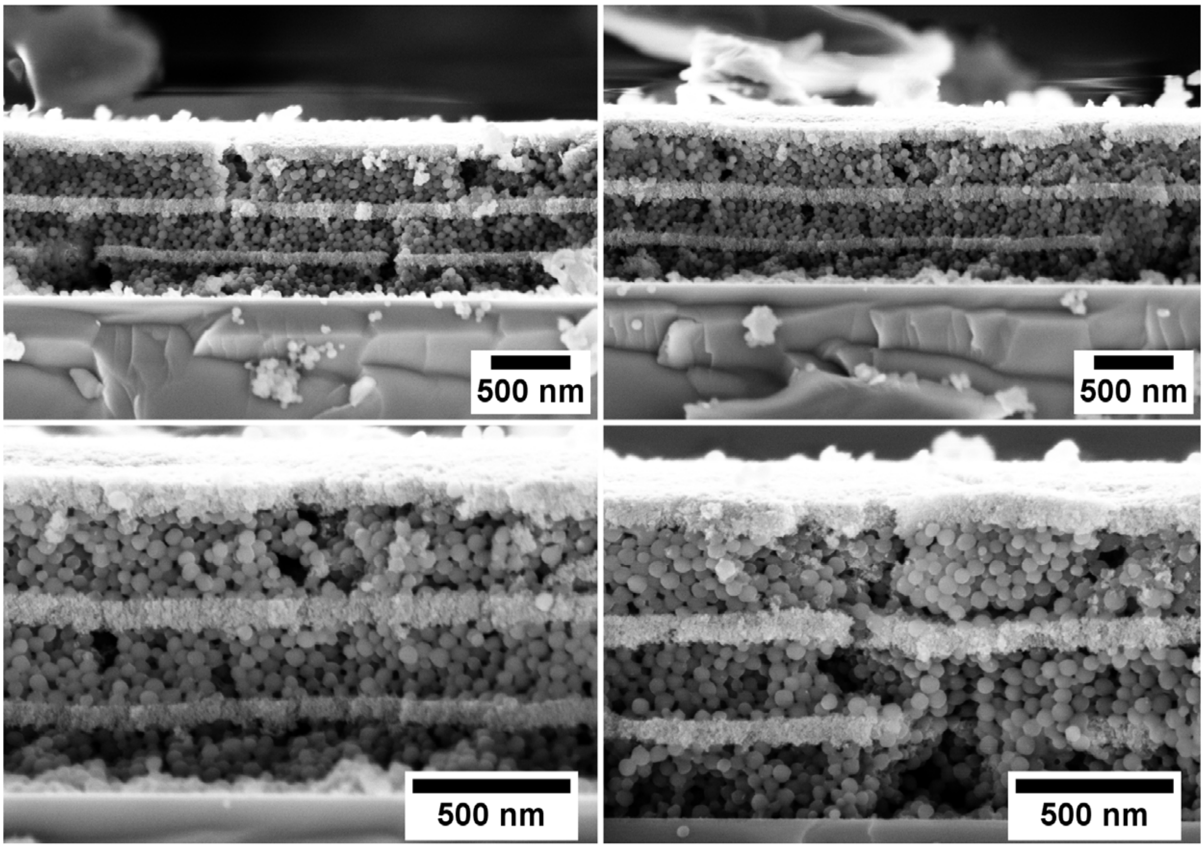

Figure S16: Scanning electron micrographs showing the 3 bilayered Bragg stack-2 with an average film thickness of ~ 50 nm for each titania layer and ~ 200 nm for each ZIF-8 layer, respectively. ZIF-8/TiO2-BS is depicted for different magnifications (x30.000 (top, left); x30.000 (top, right); x60.000 (bottom, left); x60.000 (bottom, right)).

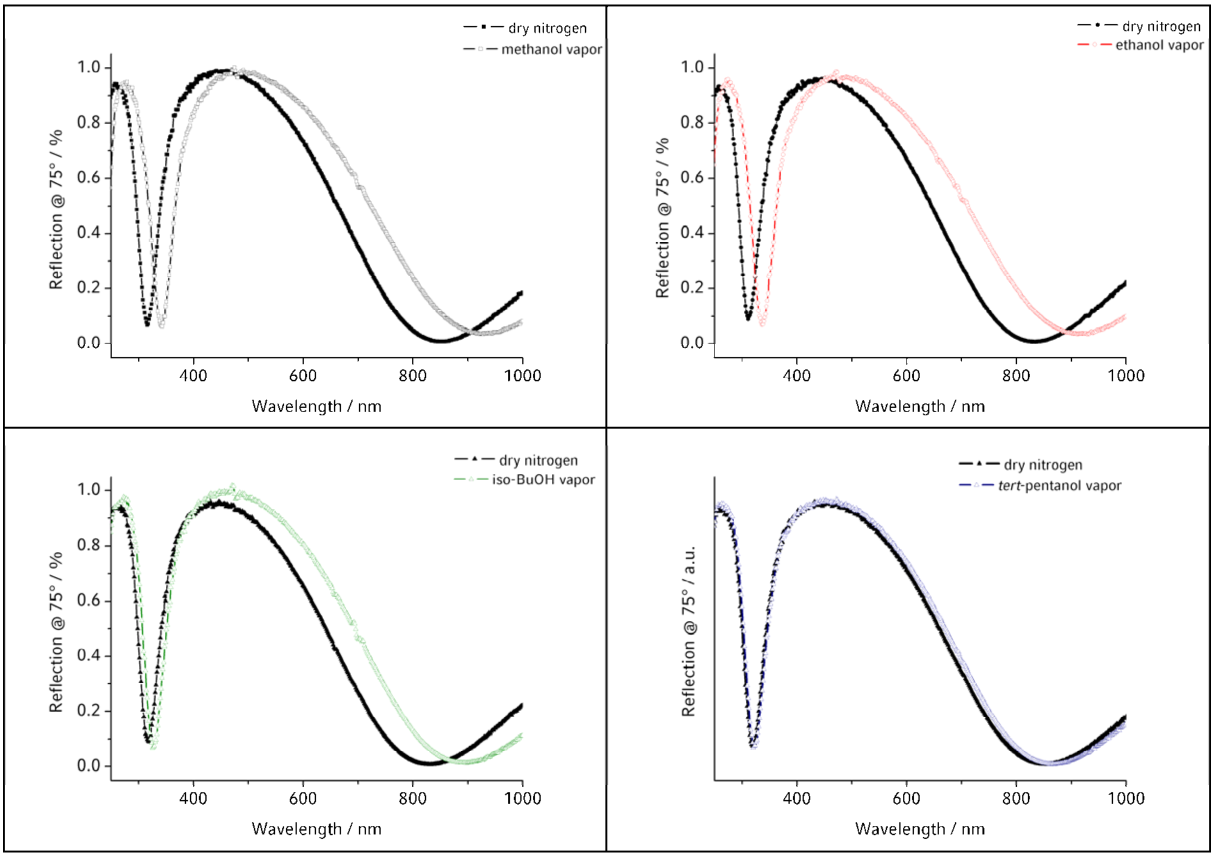

Figure S17: Reflectance spectra of a dense 200 nm single-layered ZIF-8 reference sample showing the pronounced optical shift monitored at saturation pressure upon exposure to methanol (top, left), ethanol (top, right) and *iso*-butanol (bottom, left), respectively, as well as no optical response upon *tert*-pentanol (bottom, right) sorption.

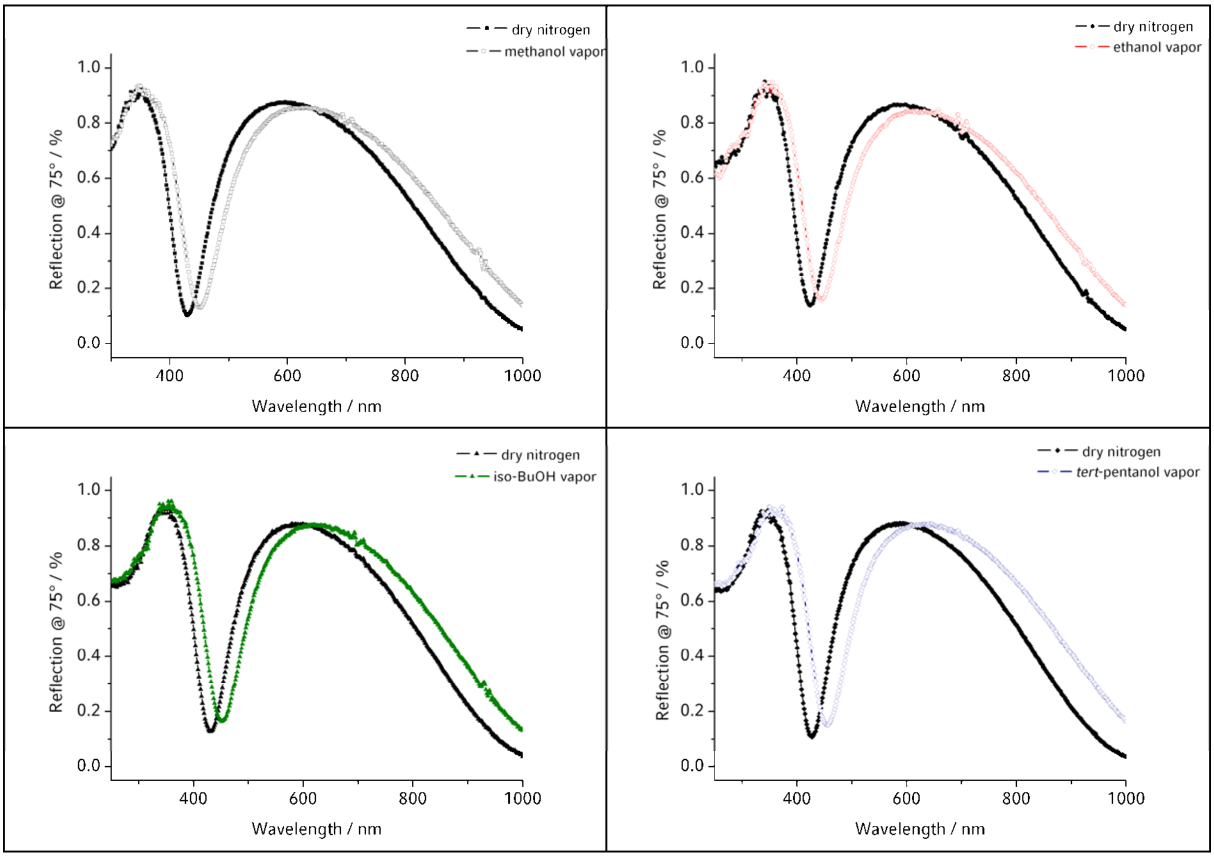

Figure S18:Reflectance spectra of the three bilayer Bragg stack 1 showing the pronounced optical shift monitored at saturation pressure upon exposure to methanol (top, left), ethanol (top, right) and *iso*-butanol (bottom, left) as well as upon *tert*-pentanol (bottom, right) sorption.

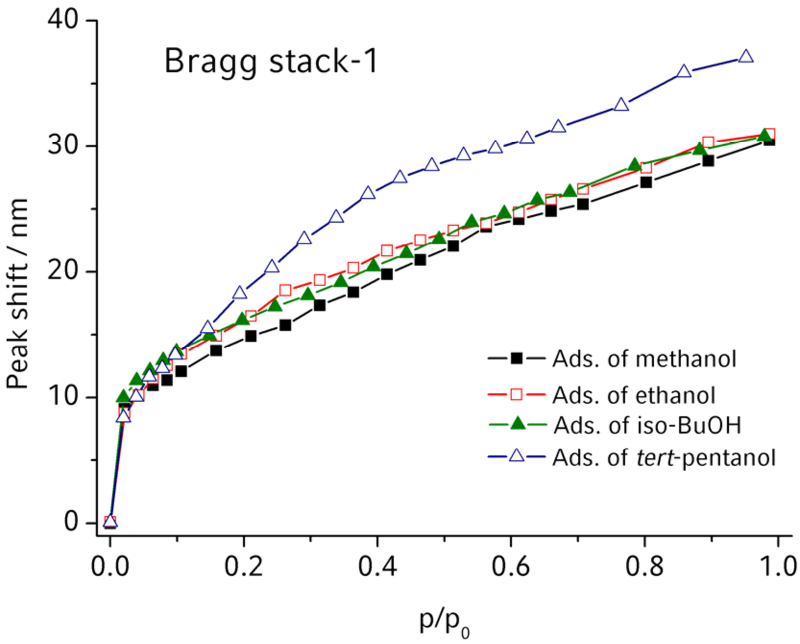

Figure S19: Optical vapor sorption isotherms demonstrating the adsorption performance of **BS-1** during exposure to a series of alcohol vapors.

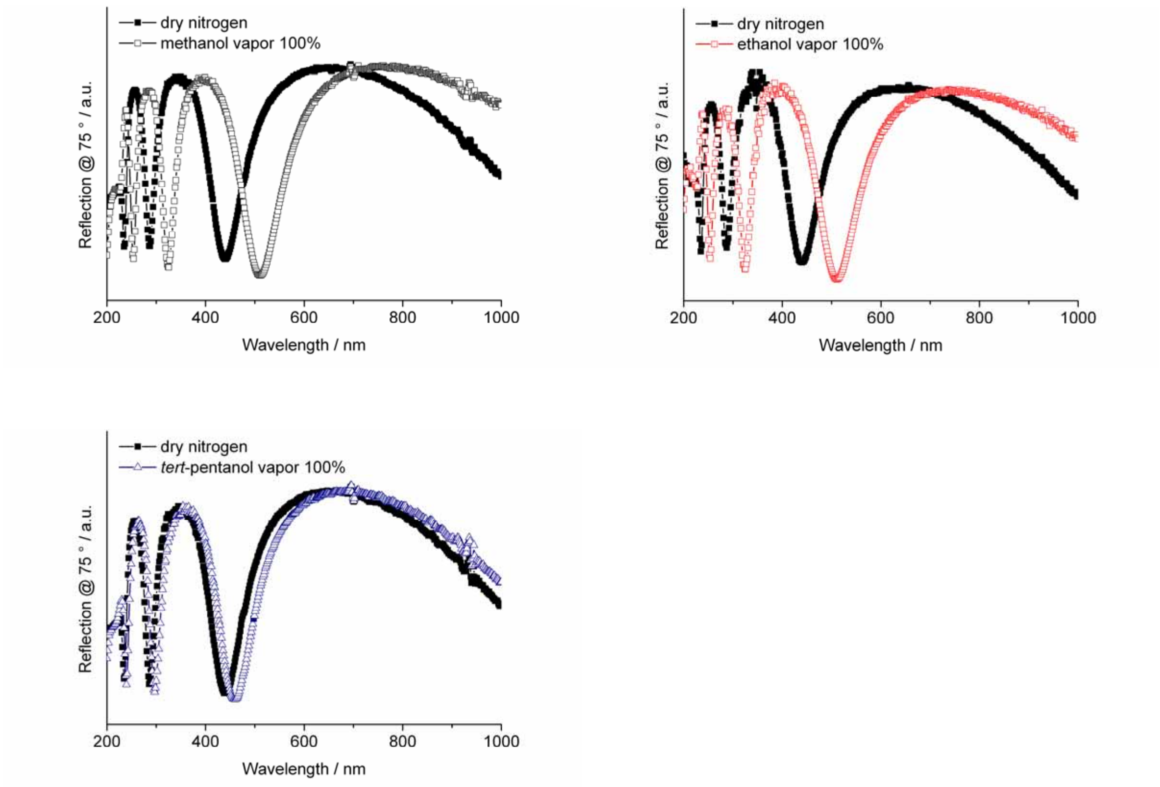

Figure S20: Reflectance spectra of a porous 400 nm single-layered ZIF-8 reference sample showing the pronounced optical shift monitored at saturation pressure upon exposure to methanol (top, left), ethanol (top, right) and *tert*-pentanol (bottom, left).

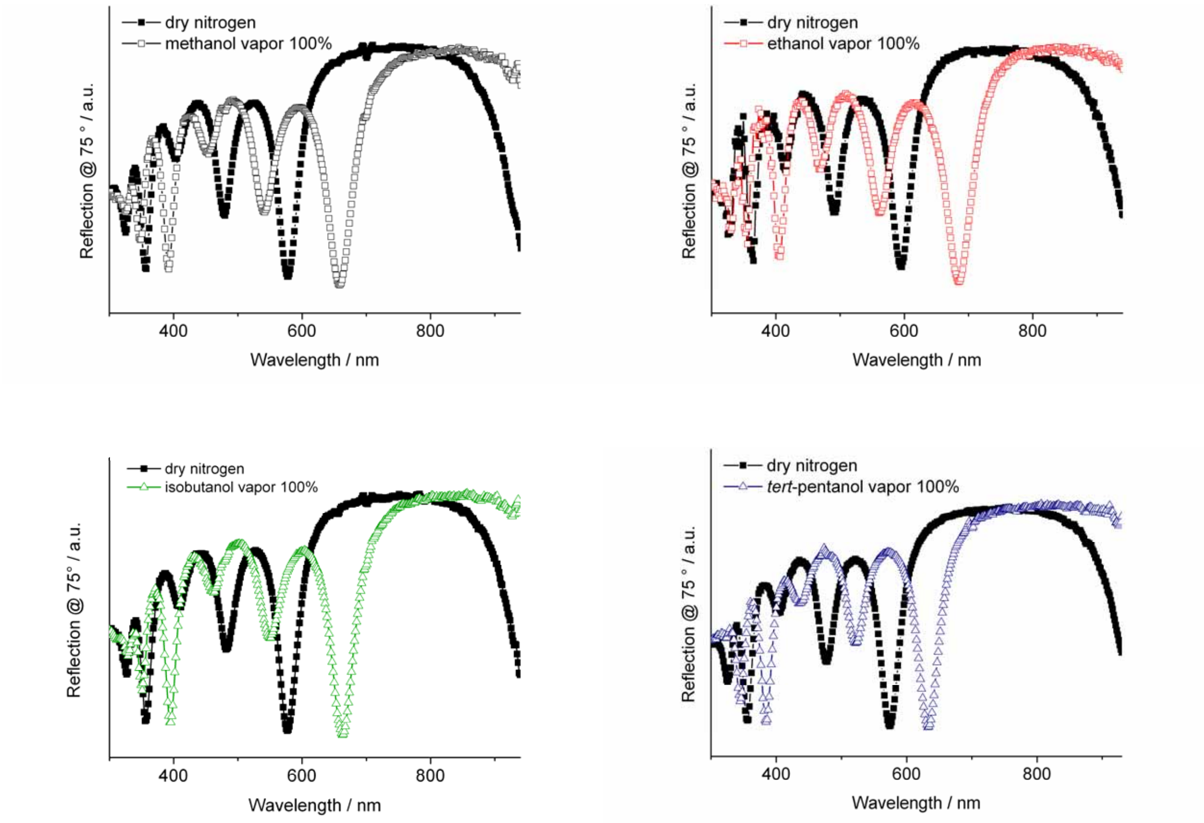

Figure S21: Reflectance spectra of the three bilayer Bragg stack 2 (DMF) showing the pronounced optical shift monitored at saturation pressure upon exposure to methanol (top, left), ethanol (top, right), isobutanol (bottom, left) and *tert*-pentanol (bottom, right).

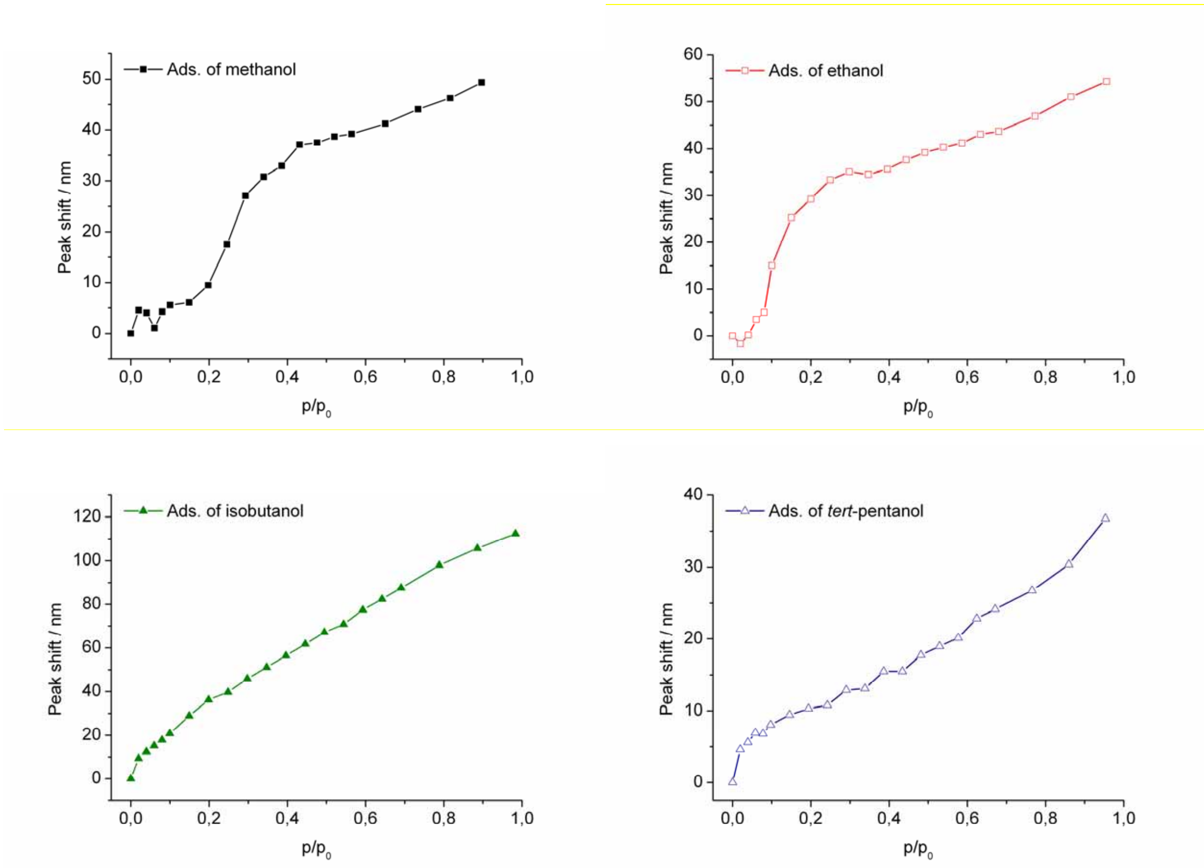

Figure S22: Reproduced optical vapor sorption isotherms demonstrating the adsorption of methanol, ethanol and *tert*-pentanol performed with Bragg stack 2 which was fabricated by redispersing the ZIF-8 nanoparticles in methanol (**BS-2** (MeOH), see Experimental Section) as well as the adsorption of isobutanol into **BS-2** prepared with nanoparticles redispersed in DMF (**BS-2** (DMF)). Owing to the different fabrication methods and the resulting differences in the ZIF-8 layer thicknesses, less pronounced absolute shifts of about 50 nm are recorded using the **BS-2** (MeOH) as compared to **BS-2** (DMF) used in Fig. 5c and for isobutanol adsorption (Fig S22). Therefore, the optical shift for isobutanol agrees well with the results obtained with **BS-2** (DMF) shown in Fig. 5c, whereas the absolute shifts for the other solvent vapors are smaller. Nevertheless, note that the shapes of all four optical isotherms are in good agreement with the isotherms shown in Fig. 5c, indicating the same host-guest interactions as in **BS-2** and thus, the same analyte selectivity to operate.